

# Patterning Self-Assembled Monolayers: Applications in Materials Science

Amit Kumar, Hans A. Biebuyck, and George M. Whitesides\*

Department of Chemistry, Harvard University, 12 Oxford Street,  
Cambridge, Massachusetts 02138

Received February 18, 1994\*

This paper describes an experimentally simple technique, based on stamping or contact printing, to pattern the adsorption of alkanethiolates on surfaces of gold, on scales from 0.2 to 100  $\mu\text{m}$ , and illustrates the use of these patterned surfaces. An elastomeric stamp, fabricated from poly(dimethylsiloxane) (PDMS), was used to deliver alkanethiol to predetermined regions of the surface of an evaporated gold film. With this technique, organic surfaces patterned with well-defined regions exhibiting different chemical and physical properties have been produced. This technique was used to pattern the adsorption of single and multiple SAMs on a single substrate. This method of preparing patterned surfaces has been used in a variety of applications, including the preparation of well-defined, heterogeneous substrates for scanning probe microscopies, the formation of microelectrodes, the formation of microstructures of silicon, the preparation of substrates for the study of condensation figures, and the preparation of substrates for patterned formation of microcrystals.

## Introduction

Self-assembled monolayers (SAMs) form when organic molecules spontaneously chemisorb on the surfaces of solids (e.g. organic thiols and disulfides on gold, silver, and copper or carboxylic acids on the surface of alumina).<sup>1,2</sup> The most robust and best characterized SAMs are those comprising alkanethiolates on gold.<sup>1</sup> By variation of the length of the alkane chain and the identity of the functional group at its terminus, the thickness of the organic layer and the chemical properties of the exposed interface can be controlled with great precision. We and others have used these SAMs for studies in tribology,<sup>3</sup> adhesion,<sup>4</sup> wetting,<sup>5</sup> and other fields.<sup>6</sup> In this paper, we describe a technique for patterning the formation of SAMs, using an elastomeric stamp, that can routinely produce patterns with dimensions from 1 to 100  $\mu\text{m}$ ; features as small as 0.2 mm (200 nm) have been generated using this procedure, although these very small features are not always easily reproduced. These patterned surfaces have geometrically well-defined regions with different chemical and physical properties. We demonstrate a number of uses for them.

## Results and Discussion

**Preparation of the Elastomeric Stamps and Formation of Patterned Surfaces.** Figure 1 diagrams the procedure for the formation of the stamp and its use to prepare patterned surfaces.<sup>7</sup> (More description is presented in the Experimental Section.) The stamp was used in conjunction with an "ink" consisting of a solution of an alkanethiol in ethanol, to print with SAMs on surfaces of gold. The stamp was fabricated by casting poly(dimethylsiloxane) (PDMS) on a master having the desired features. We used several types of masters for the fabrication of stamps: commercially available transmission electron microscopy grids, structures prepared photolithographically by exposing and developing a photoresist pattern on a solid support (typically a silicon wafer), and semiconductor wafers that have been processed photolithographically and metalized. After curing, the PDMS stamp was peeled away from the master. The master could be reused a number of times to produce multiple copies of the stamp. Figure 1b shows a photograph of a representative stamp. The square, opaque area is the region that contains the desired microscopic features. Figure 1c shows a magnified view of the features on a representative stamp. This stamp was exposed to an ethanolic solution (1–10 mM) of the alkanethiol that was to be patterned on the surface. We believe that the PDMS swelled slightly upon exposure to the solution.<sup>8</sup> The thiol was transferred to the surface by bringing the stamp and the gold into contact. Although the surface of the gold was not smooth on a molecular scale (these evaporated films typically have corrugations of 50–100 Å), the elastomeric nature of PDMS allowed for conformal contact between the stamp and the surface. After removal of the stamp, the gold surface could be used in studies where single, patterned SAMs were desired. Alternatively, the gold could be exposed to a solution of another alkanethiol or dialkyl disulfide to derivatize the remaining bare regions

\* To whom correspondence should be addressed.

† Abstract published in *Advance ACS Abstracts*, April 1, 1994.

(1) Nuzzo, R. G.; Allara, D. L. *J. Am. Chem. Soc.* **1983**, *105*, 4481. Troughton, E. B.; Bain, C. D.; Whitesides, G. M.; Nuzzo, R. G.; Allara, D. L.; Porter, M. D. *Langmuir* **1988**, *4*, 365.

(2) Laibinis, P. E.; Hickman, J.; Wrighton, M. S.; Whitesides, G. M. *Science (Washington, DC)* **1989**, *245*, 845.

(3) Salmeron, M. B. *MRS Bull.* **1993**, *18*, 20–25.

(4) Allara, D. L.; Hebard, A. F.; Padden, F. J.; Nuzzo, R. G.; Falcone, D. R. *J. Vac. Sci. Technol. A* **1983**, *376*. Haussling, L.; Ringsdorf, H.; Schmitt, F. J.; Knoll, W. *Langmuir* **1991**, *7*, 1837.

(5) Bain, C. D.; Whitesides, G. M. *J. Am. Chem. Soc.* **1988**, *110*, 6560. Bain, C. D.; Whitesides, G. M. *J. Am. Chem. Soc.* **1989**, *111*, 7155. Bain, C. D.; Whitesides, G. M. *J. Am. Chem. Soc.* **1988**, *110*, 3665. Bain, C. D.; Whitesides, G. M. *Science (Washington, DC)* **1988**, *240*, 62. Bain, C. D.; Whitesides, G. M. *J. Am. Chem. Soc.* **1989**, *111*, 7164.

(6) See for example Black, Andrew J.; Wooster, Timothy T.; Geiger, William E. *J. Am. Chem. Soc.* **1993**, *115*, 7924–5. Duerig, U.; Zueger, O.; Michel, B.; Haeussling, L.; Ringsdorf, H. *Phys. Rev. B* **1993**, *8*, 1711–17. Willner, Itamar; Rubin, Shai; Cohen, Yael. *J. Am. Chem. Soc.* **1993**, *115*, 4937–8. Ong, T. Hui; Davies, Paul B.; Bain, Colin D. *Langmuir* **1993**, *9*, 1836–45. Huang, Jingyu; Hemminger, John C. *J. Am. Chem. Soc.* **1993**, *115*, 3342–3. Stenger, David A.; Georger, Jacques H.; Dulcey, Charles S.; Hickman, James J.; Rudolph, Alan S.; Nielsen, Thor B.; McCort, Stephen M.; Calvert, Jeffrey M. *J. Am. Chem. Soc.* **1992**, *114*, 8435–42.

(7) Kumar, A.; Whitesides, G. M. *Appl. Phys. Lett.*, in press.

(8) We believe the swelling of the polymer did not distort the features.

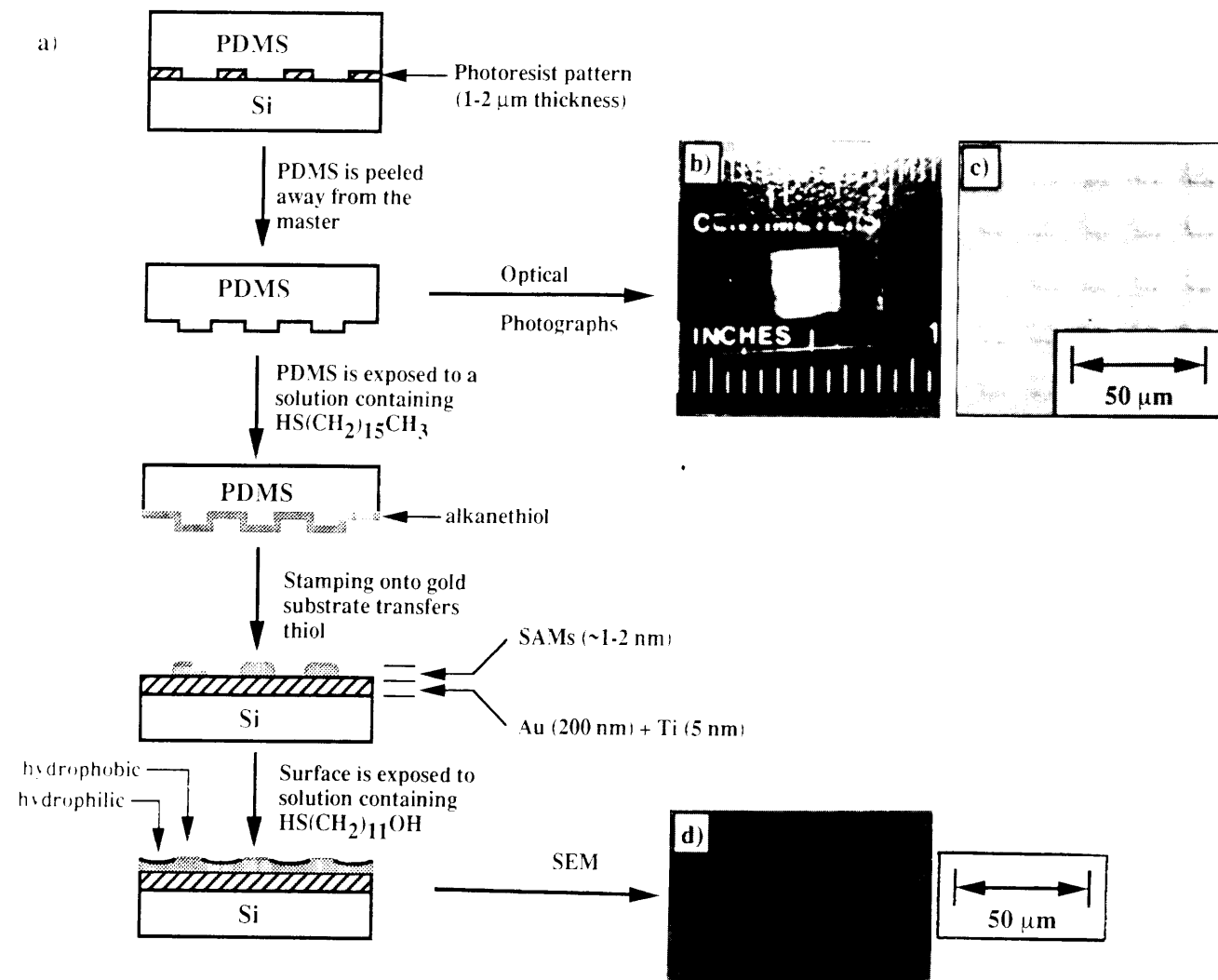


**Figure 1.** Procedure for fabrication of the patterned elastomeric stamp, and for preparation of patterned surface. (a) An exposed and developed photoresist pattern on a silicon wafer was used as the master. Poly(dimethylsiloxane) (PDMS) was polymerized on the master and carefully peeled away. The stamp was inked by exposure to an ethanolic solution (1–10 mM) of the appropriate alkanethiol, brought into contact with the gold substrate, and removed. The substrate was then washed for 2–4 s with a solution of another alkanethiol (1–10 mM in ethanol). The substrate was finally washed for 10 s with ethanol and dried in a stream of nitrogen. (b) Photograph of a stamp. The region with the features are in the square section. (c) A magnified view of the features in the square section. (d) This electron micrograph is representative of a patterned surface. The stamp having square features, 10 μm on a side, was used to pattern the adsorption of  $\text{HS}(\text{CH}_2)_{15}\text{CH}_3$  on the gold (light regions); the gold was subsequently exposed to  $\text{HS}(\text{CH}_2)_{10}\text{CH}_2\text{OH}$  (dark regions).

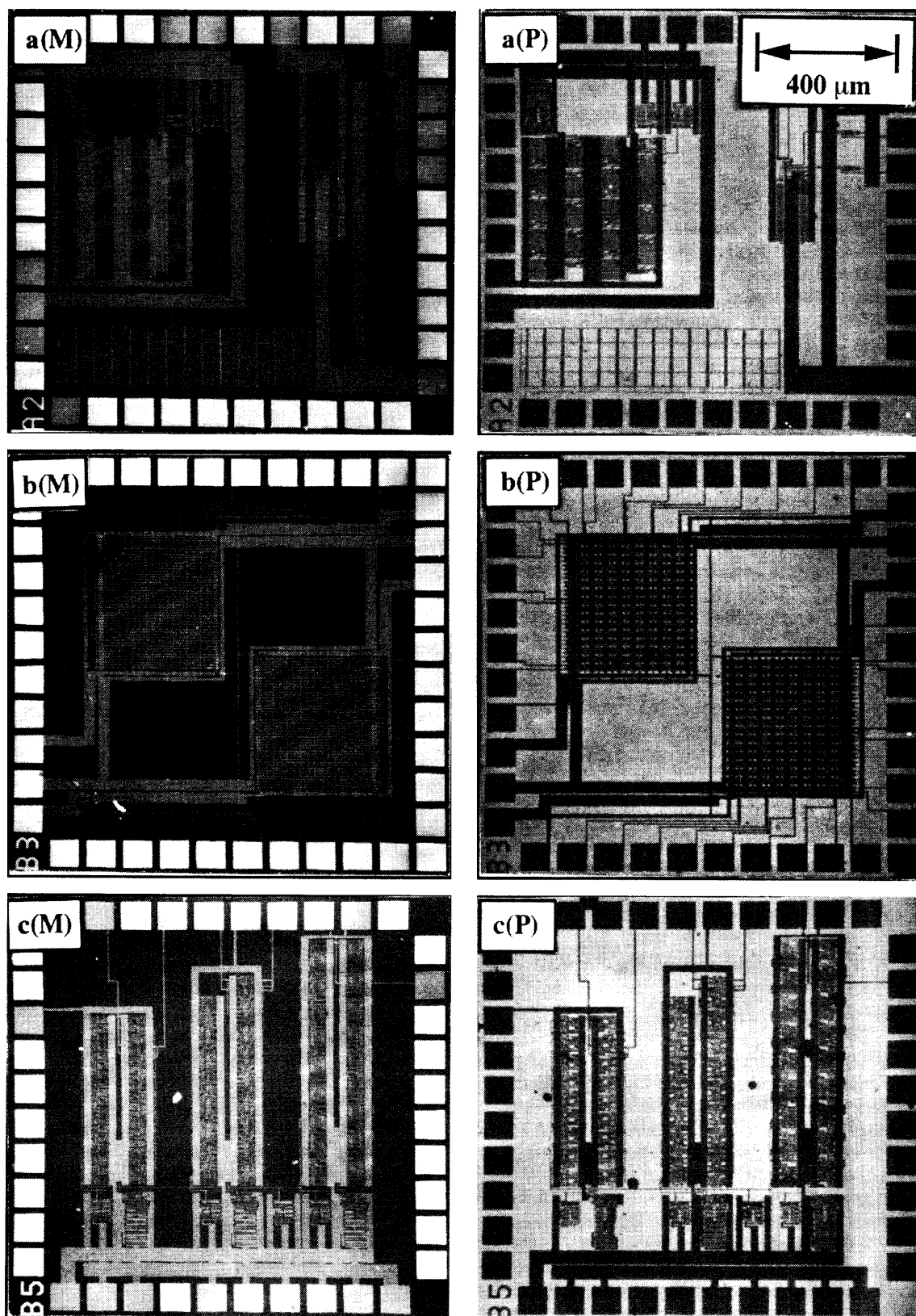
with a second SAM. Multiple printing steps with the same stamp (we have used the same stamp up to 100 times over a period of several months with no evidence of loss of performance), with different stamps, and with different alkanethiols could be carried out on a single substrate. This flexibility made it straightforward to prepare a range of surfaces having both simple and complex patterns consisting of one or several SAMs, using simple stamps.

Figure 1d shows a scanning electron micrograph (SEM) of a representative surface. A stamp having squares 10 μm on a side (shown in Figure 1b,c) was used to stamp a pattern of  $\text{HS}(\text{CH}_2)_{15}\text{CH}_3$  (light) on gold, and the remaining regions were exposed to  $\text{HS}(\text{CH}_2)_{10}\text{CH}_2\text{OH}$  (dark). The micrograph shows that the edge resolution is on the submicrometer scale, but it is not clear whether the boundary between SAMs is abrupt on molecular dimensions. We believe that the contrast observed in this image is primarily due to attenuation of secondary electrons by impurities adsorbed on the SAMs. More contaminants adsorb onto the high free energy surfaces that form when SAMs are made from alkanethiols with terminal hydroxyls (and other hydrophilic functionalities) than on SAMs

prepared from alkanethiols with terminal methyls; consequently, the hydrophilic regions appear darker.<sup>9</sup>

Parts a(M), b(M), and c(M) of Figure 2 show several SEMs of complex microelectronic patterns that were produced using conventional lithography. These structures were used in turn as masters to produce stamps, which reproduced corresponding patterns in SAMs of  $\text{HS}(\text{CH}_2)_{15}\text{CH}_3$  on gold surfaces. The SAMs formed from  $\text{HS}(\text{CH}_2)_{15}\text{CH}_3$  were hydrophobic, low free-energy surfaces. The patterned gold was washed with an ethanolic solution (1–10 mM) of  $\text{HS}(\text{CH}_2)_{10}\text{CH}_2\text{OH}$  to functionalize the bare regions. Parts a(P), b(P), and c(P) of Figure 2 show the fidelity with which the original masters are replicated in the final imprinted patterns. In parts a(M), b(M), and c(M) of Figure 2 the features that appear lighter are features that are physically raised higher than the features that appear darker. When stamps were made using these microelectronic structures as masters, the raised regions of the master corresponded to the recessed regions of the stamp. When such stamps were inked with  $\text{HS}(\text{CH}_2)_{15}\text{CH}_3$

(9) Lopez, G. P.; Biebuyck, H. A.; Whitesides, G. M. *Langmuir* **1993**, *9*, 1513.



**Figure 2.** SE micrographs of masters formed using conventional microlithography, a(M), b(M), and c(M), and the patterned surfaces, a(P), b(P), and c(P) produced using stamps formed on the masters. The masters were produced through several conventional lithographic steps involving oxidizing and coating substrates, photolithography, etching, metalization, and lift-off; the exact details of these processes seem not to influence the stamp. These masters had a relief in their features of thickness between 0.8 and 1.5  $\mu\text{m}$ . Rubber stamps were used to pattern the adsorption of  $\text{HS}(\text{CH}_2)_{15}\text{CH}_3$  (light regions). The surfaces were then washed with ethanolic solutions of  $\text{HS}(\text{CH}_2)_{10}\text{CH}_2\text{OH}$  (dark regions). Since the stamped regions appear bright, the patterned surfaces are direct negative images of the corresponding masters. The resolution of these features and others in this paper is below 1  $\mu\text{m}$ . The purpose of this figure is to show the complexity of features that can be produced through stamping.

$\text{CH}_3$  and brought into contact with gold surfaces, a negative, hydrophobic pattern of the original master was produced on the surface (see Figure 1a). After washing

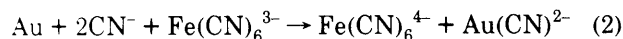
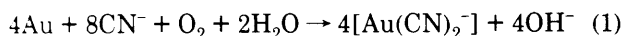
with a solution of  $\text{HS}(\text{CH}_2)_{10}\text{CH}_2\text{OH}$ , the underivatized regions of the surface, corresponding to the bright regions of the original masters, were functionalized with a

hydrophilic SAM. Since the SAMs formed from HS-(CH<sub>2</sub>)<sub>15</sub>CH<sub>3</sub> appear bright in the electron micrographs, and the SAMs formed from HS(CH<sub>2</sub>)<sub>10</sub>CH<sub>2</sub>OH appear dark, the pictures in parts a(P), b(P), and c(P) appear as direct negatives of the structures shown in parts a(M), b(M), and c(M).

Close inspection of the stamped patterns, a(P), b(P), c(P), shows that there are some small areas that were not directly replicated from the masters. These areas of imperfection resulted from our relatively crude method of stamping. All of the mechanical stamping steps for this paper were done by hand. Presumably, a more precise method using instrumentation would produce even better results than those described in this work. For the purpose of this paper—to demonstrate the principle of this method—stamping by hand was sufficient.

The most attractive features of patterning the formation of SAMs using the rubber stamping technique is the simplicity of the procedure and the great fidelity of the transfer of the pattern. Once a master has been prepared and a corresponding stamp has been fabricated, multiple impressions can be made routinely and quickly without further access to lithographic facilities. The microscopic features on the PDMS stamps produced in this manner do not appear to degrade with time or use. Further, the patterned surfaces produced through this technique are extremely robust. Samples, that had been exposed to the laboratory ambient for periods greater than 9 months, exhibited no detectable degradation. These surfaces could be repeatedly washed vigorously with polar and nonpolar liquids, and dried in flowing streams of gases without being damaged. The following sections describe several applications of surfaces that have been patterned with SAMs using rubber stamps.

**Preparation of Microstructures of Gold.** When clean gold is exposed to an aqueous solution of cyanide ion in the presence of a mild oxidant, such as dioxygen or ferricyanide, the gold dissolves.<sup>10,11</sup> The free energy of this process is dominated by the formation of the very stable Au(CN)<sub>2</sub><sup>-</sup> ion.



A SAM composed of hexadecanethiolate protects the gold from dissolving in this corrosive medium.<sup>7,12</sup> Figure 3 shows an example of the protecting ability of a hexadecanethiolate SAM on gold. (The gold layer was 1 μm thick on a Ti primed Si wafer.) The region that was protected by the thiolate layer was not etched while the bare region was etched completely as indicated by the lack of a gold signal using energy dispersive X-ray spectroscopy. The morphology at the edge of the gold layer is characteristic of most wet chemical etches for metals.

By patterning the adsorption of hexadecanethiolate on gold using the rubber stamp, and by subsequently etching the surface in a solution of cyanide ion (1 M KOH, 0.1 mM KCN, saturated with oxygen, 20–25 °C), microstructures of gold were easily produced. Using this procedure, we have made many types of features having dimensions from 0.2 μm to several hundred μm; Figure 4 and Figure 5 show

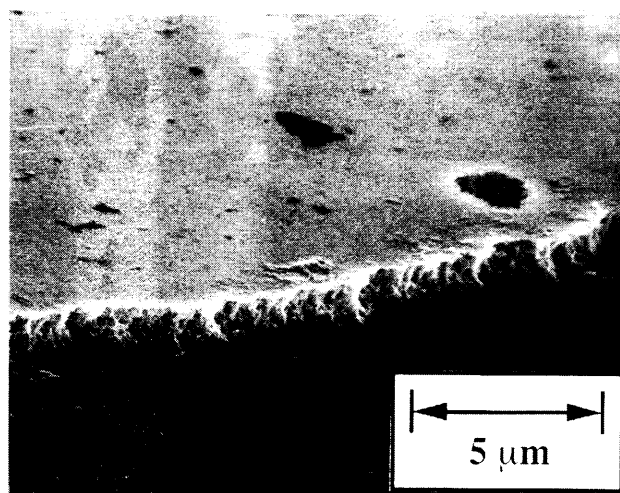


**Figure 3.** An example of the protecting ability of a SAM. A gold layer (1 μm thick) was deposited on a Ti-primed (50 Å thick) silicon wafer. The top region was exposed to a solution of HS-(CH<sub>2</sub>)<sub>15</sub>CH<sub>3</sub> in ethanol. The lower region was bare gold. This surface was immersed in a 1 M KOH solution with 1 mM KCN. Oxygen was bubbled continuously through the solution. The region protected by the SAM was not etched, while the bare gold completely dissolved. The thickness of the unetched gold was the same before and after etching (as determined using profilometry). The monolayer was still intact as determined by contact angle measurements. The dark spots on the unetched gold are particles or oil spots, not etch pits; they coincidentally appear dark by electron microscopy.

representative SEMs of some structures that were produced through this procedure. Figure 4 shows an etched pattern (of the type used in the fabrication of microelectronic devices) having four quadrants. Magnified views of each quadrant are also shown. Figures 5a–d show various other device patterns with their associated interconnections and contact pads. Figure 5e is a fracture profile of a series of gold microwires. The fractured and tilted view is useful for visualization of the depth of the gold (0.2 μm thick) on silicon. Figure 5f demonstrates the best resolution that we have so far obtained using the rubber stamping technique. This panel shows a series of parallel lines that are 0.2 μm wide.<sup>13</sup> Structures of this size indicate that this technique can be useful for producing features that are normally fabricated using electron-beam lithography and X-ray lithography.

Most of the etching experiments were conducted using SAMs formed from HS(CH<sub>2</sub>)<sub>15</sub>CH<sub>3</sub> as the resist, although SAMs formed from alkanethiols having longer chains provided comparable protection from etching. Shorter chain alkanethiols provided some degree of protection, but their ability to resist etching decreased with decreases in the length of the chain. The terminal functionality of the thiol incorporated in the monolayer also affected the quality of the resist. In general, SAMs comprising nonpolar, methyl-terminated thiols exhibited the greatest resistance to etching, while those terminated in polar functionalities such as hydroxyl and carboxylic acid groups had poorer resistance. SAMs prepared from thiols having fluoroalkyl functionalities in their chains or termini exhibited etch protection comparable to or better than SAMs of corresponding thickness prepared from simple alkanethiols. These studies suggest that a primary characteristic that determines the effectiveness of the resist is the ability of the SAM to exclude penetration of cyanide ions through the SAM to the surface of gold.

(10) Brittan, A. M. *Am. Sci.* **1974**, *62*, 402. Puddephatt, R. J. *The Chemistry of Gold*; Elsevier: Amsterdam, 1978.

(11) Cotton, F. A.; Wilkinson, G. *Advanced Inorganic Chemistry*, 4th ed.; Wiley: New York, 1980; p 966.

(12) Kumar, A.; Biebuyck, H. A.; Abbott, N. L.; Whitesides, G. M. *J. Am. Chem. Soc.* **1992**, *114*, 9188.

(13) The masters for submicrometer structures were produced by X-ray lithography by Henry Smith of the Massachusetts Institute of Technology.

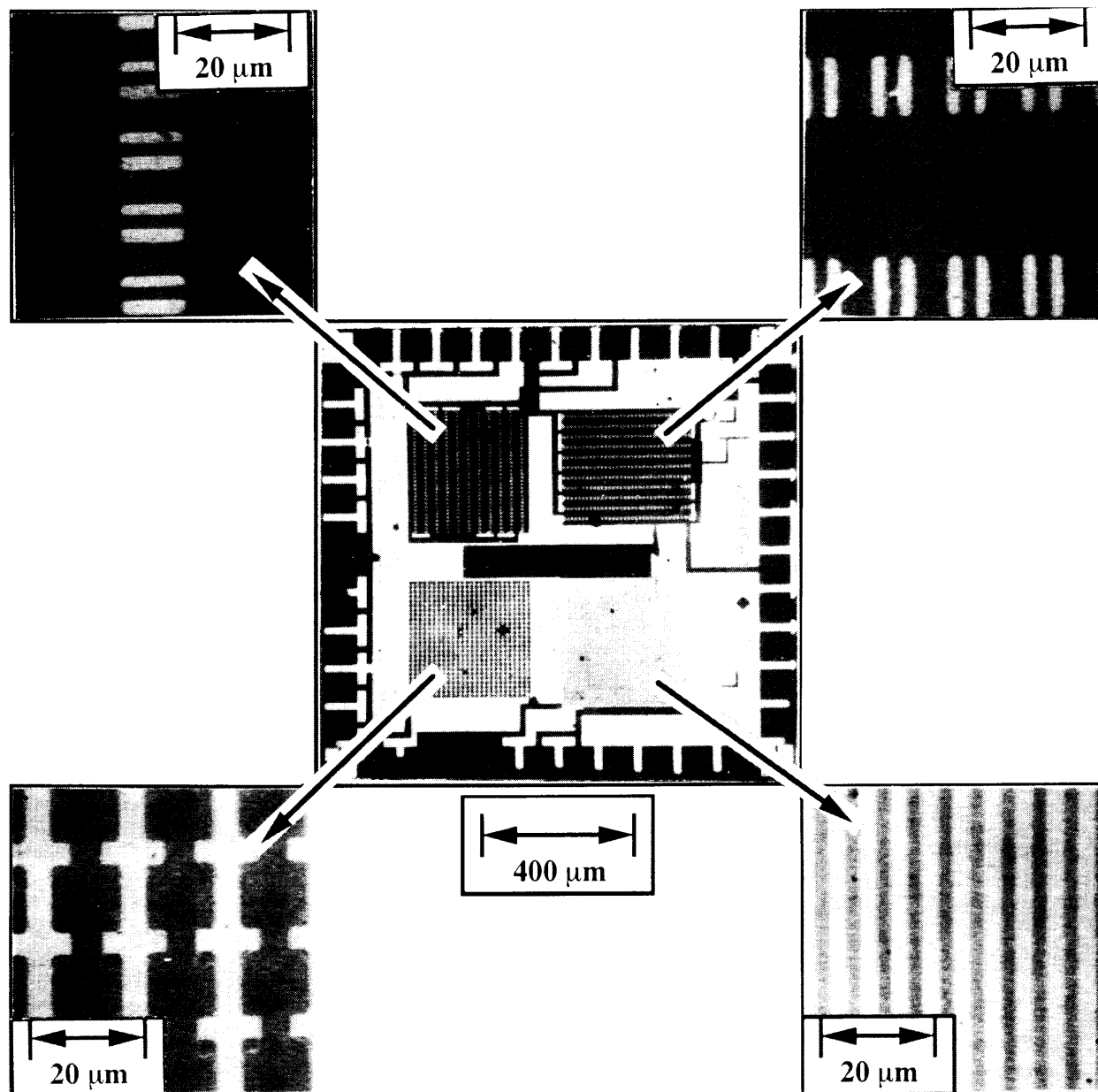


**Figure 4.** SE micrographs of various types of features produced using rubber stamping and chemical etching. The central device is a structure with four different quadrants. A magnified view of each quadrant is shown.

A diagnostic of the protecting ability of SAMs was the number of defects (etch pits) observed over the regions of gold that were derivatized. For the best cases, we observed, by SEM, 5 pits/mm<sup>2</sup> over protected regions of gold.<sup>12</sup> These pits were circular with diameters between 0.5 and 1.0 μm; SEM allowed us to view to resolve crystallites in the gold that were 50–100 nm in diameter. Considering the thickness of the resist (one molecular layer, ~12 Å), this density of pits is low; by the standards of microelectronics fabrication, 5 pits/mm<sup>2</sup> is too high for most applications.<sup>14</sup> It is not clear whether the origins of the pits are inherent defects at the molecular level in the monolayer itself or adsorbed contaminants and dust particles that produce defects on a larger scale in the monolayer. Preliminary studies indicate that the density of pits can be reduced (by at least factors of 2 to 5) by conducting the experiments under clean room conditions. These experiments suggest

that the origins of the defects are, at least in part, adsorbed contaminants or dust particles.

The toxicity of the cyanide-based solution was a concern. We examined other, less toxic solutions that provided selective etching characteristics comparable to the cyanide solution. Table 1 summarizes these formulations. The adsorption of CN<sup>-</sup> on metals, especially Au, can decrease their oxidation potentials by up to 2 V.<sup>10,15</sup> Chemisorption of sulfur compounds such as thiols also decreases the oxidation potential of Au, but the magnitude of decrease for thiol compounds is not as great as that for cyanide ion.<sup>10,15</sup> In regions where the Au is derivatized with an alkylthiolate, cyanide cannot adsorb, and these protected regions dissolve at very low rates compared to underivatized gold: Cyanide cannot readily penetrate the low dielectric, alkyl chain environment of these SAMs so that the underlying gold remains because of this kinetic barrier to mass transport to the surface. Considering the properties of the etch solution based on cyanide ion, there are two

(14) Muller, R. S.; Kamins, T. J. *Device Electronics for Integrated Circuits*, 2nd ed.; Wiley: New York, 1986. Van Zant, P. *Microchip Fabrication: A Practical Guide to Semiconductor Processing*, 2nd ed.; McGraw-Hill: New York, 1990.

(15) McCarley, R. L.; Kim, Y. T.; Bard, A. J. *J. Phys. Chem.* **1993**, *97*, 211–215.



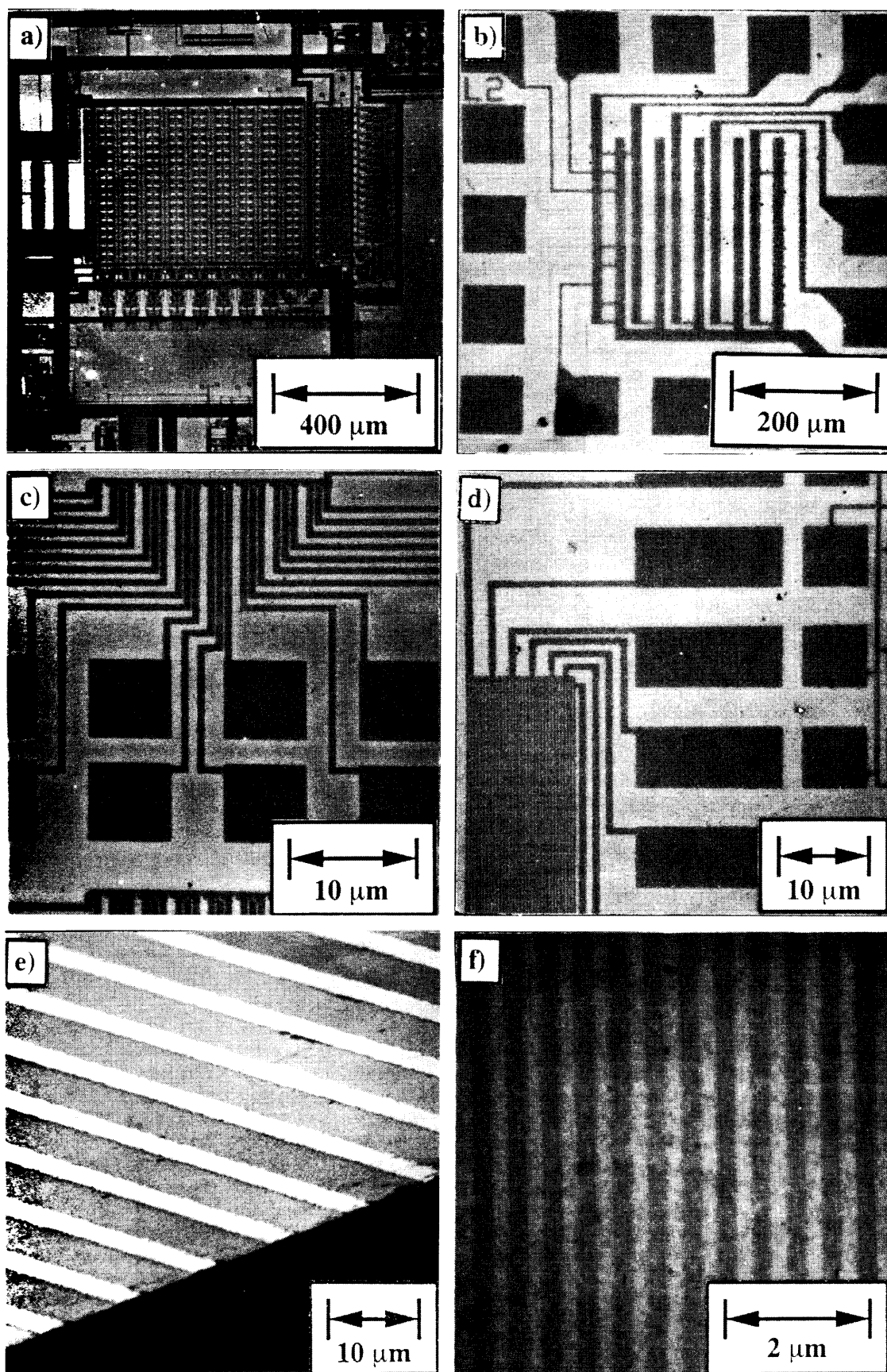


**Figure 5.** SE micrographs of several types of structures formed through rubber stamping and chemical etching (a–d). (e) Fracture profile of a series of gold lines supported on a silicon wafer. The width of the gold lines is  $2\ \mu\text{m}$ , and the thickness of the gold is  $2000\ \text{\AA}$ . The tilt allows observation of the thickness of the gold and the resolution of the edge. (f) The smallest features that are currently accessible using rubber stamping. The width of the lines is  $0.2\ \mu\text{m}$ . Although the arrays with features on scales of  $1\ \mu\text{m}$  or greater are easy to produce, the arrays of submicrometer ( $0.2\ \mu\text{m}$ ) lines are not routinely reproducible through rubber stamping by hand: they represent best-case examples, and the view shown was chosen from regions of lower fidelity. More precise mechanical control should allow these arrays to be produced with better reproducibility.

**Table 1. Summary of Etching**

| oxidant                                       | electrolyte  | comments <sup>a</sup> |
|---|--|-----------------------|
| K <sub>3</sub> Fe(CN) <sub>6</sub> (0.001 M)  | KCN (0.1 M)  | selective             |
| O <sub>2</sub>                                | KCN (0.1 M)  | selective             |
| O <sub>2</sub>                                | KCN (0.001 M)  | selective             |
| K <sub>3</sub> Fe(CN) <sub>6</sub> (0.0001 M) | KSCN (0.1 M)   | selective             |
|   | 1.0 M KOH  |                       |
| K <sub>3</sub> Fe(CN) <sub>6</sub> (0.01 M)   | K <sub>2</sub> S <sub>2</sub> O <sub>3</sub> (0.1 M) | selective             |
|   | 1.0 M KOH  |                       |
| O <sub>2</sub>                                | KSCN (0.1 M)   | etching slow          |
|   | 1.0 M KOH  |                       |
| O <sub>2</sub>                                | K <sub>2</sub> S <sub>2</sub> O <sub>3</sub> (0.1 M) | etching slow          |
|   | 1.0 M KOH  |                       |
| H <sub>2</sub> O <sub>2</sub> (30%)           | KCl (0.1 M)  | no selectivity        |
| I <sub>2</sub> (0.025 M)                      | KI (0.16 M)  | no selectivity        |
| HCl:HNO <sub>3</sub> (concentrated)           | aqua regia   | no selectivity        |
| K <sub>3</sub> Fe(CN) <sub>6</sub> (0.01 M)   | NaCl (1.0 M)   | no etching            |
| K <sub>3</sub> Fe(CN) <sub>6</sub> (0.01 M)   | KI (0.1 M)   | no etching            |
| FeCl <sub>3</sub> (0.01 M)                    | KI (0.1 M)   | no etching            |
| O <sub>2</sub>                                | squaric acid   | no etching            |
|   | 1.0 M KOH  |                       |
| K <sub>3</sub> Fe(CN) <sub>6</sub> (0.01 M)   | squaric acid   | no etching            |
|   | 1.0 M KOH  |                       |

<sup>a</sup> These etching studies were conducted on substrates of gold. Metrics for entries in this column are as follows: no etching, on a time scale of minutes; no etching was observed by eye; no selectivity, on a time scale of minutes, both derivatized and underivatized regions of the gold dissolved; slow etching, selective etching was observed, but the rate was slow (less than 100 Å/h); selective, on a time scale of minutes, only underivatized regions of gold dissolved. (See text for further discussion.)

key requirements for selective etching. First, the etch solution must contain a coordinating ion that does not disrupt the alkanethiolate monolayer and that, through adsorption to the bare gold surface, decreases the oxidation potential of gold. Second, it must include an oxidant that does not disrupt the SAM but oxidizes bare gold in the presence of this coordinating ion. The latter property can be due to a combination of the redox potential of the oxidant and the impermeability of the SAM to the oxidant. Oxygen and ferricyanide (under certain conditions) are such oxidants.<sup>16</sup>

Coordinating ions such as Cl<sup>-</sup> and I<sup>-</sup> do not reduce the oxidation potential of gold significantly. Therefore, mild oxidants such as ferric ion, ferricyanide, or oxygen do not have sufficiently positive oxidation potentials to oxidize gold in the presence of these halides. In the presence of these ions gold can only be oxidized by strong oxidizing agents such as hydrogen peroxide, iodine, chlorine, etc.<sup>17</sup> These oxidizing agents oxidize both bare gold and gold that is derivatized with a SAM at comparable rates: little or no selectivity in etching is observed for such solutions under the conditions we surveyed.

Adsorption of thiocyanate and thiosulfate on Au has an effect similar to that of cyanide, although the magnitude of decrease of the Au oxidation potential is not as large.<sup>15</sup> In solutions of thiocyanate or thiosulfate where dioxygen is the oxidant, selectivity in etching is observed, but the rate of dissolution of gold is slow. In such electrolytes, with ferricyanide as the oxidant at a relatively high concentration (0.01 M), selectivity in etching comparable to that found for the cyanide-based etch and useful dissolution rates of gold (1–3 Å/s) are observed. In the best cases, no etching of protected gold was observed even after 12 h in the etch bath.

Most of the selective etching work reported in this paper was conducted on surfaces of gold patterned with SAMs,

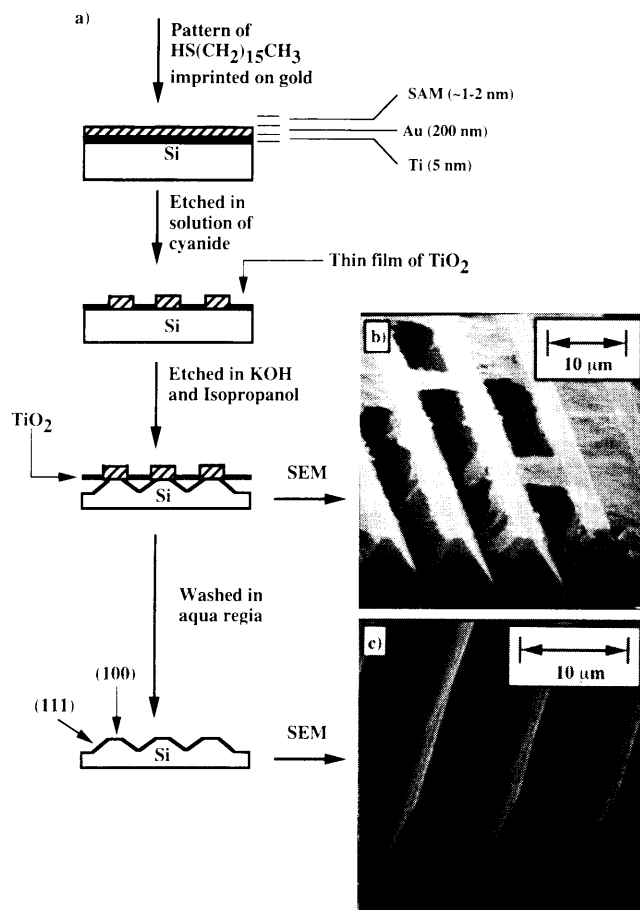


**Figure 6.** Formation of features produced by using microstructures of gold as masks for etching of silicon. (a) Schematic representation of the procedure. A stamp consisting of parallel lines of 2 μm width was used in combination with wet etching in a cyanide solution to produce the gold mask. (b) Grooves of silicon were formed using an anisotropic etch (2 M KOH, 15% 2-propanol by volume) for silicon. The (100) face etches faster than the (111) face. A thin, porous film of titanium dioxide remained. (c) Washing the structure with aqua regia (3:1 concentrated HCl:HNO<sub>3</sub>) removed the film and exposed the morphology of the grooves.

although comparable data were also obtained for patterned surfaces of silver or copper. These studies indicate that a combination of rubber stamping, to pattern the adsorption of molecules on metals, and selective chemical etching can be useful for the production of complex metal structures on a scale comparable to UV photolithography.<sup>14</sup> In some cases, features on scales comparable to those commonly produced by electron-beam lithography and X-ray lithography can be achieved.<sup>14</sup>

**Etching of Silicon.** Once the microstructures of gold have been produced on silicon substrates as described above, the gold itself can be used as a resist for anisotropic etching of silicon. Figure 6 depicts the process and shows SEMs of corresponding structures. The (100) face of silicon is more reactive than the (111) face, and anisotropic etches take advantage of this characteristic.<sup>18</sup> For example, a solution of hydroxide ion and an alcohol such as 2-propanol will etch the (100) face at a rate that is 2 orders of magnitude faster than the (111) face.<sup>19</sup>

Our wafers were cut and polished with the (100) face exposed. After forming lines of gold on the surfaces of

(16) Other mild oxidants in addition to oxygen or ferricyanide should also produce selective etching.

(17) Bard, A. J.; Faulkner, L. R. *Electrochemical Methods: Fundamentals and Applications*; Wiley: New York, 1980.

(18) Seidel, H.; Csepregi, L.; Heuberger, A.; Baumgaertel, H. *J. Electrochem. Soc.* **1990**, *137*, 3612–26. Seidel, H.; Csepregi, L.; Heuberger, A.; Baumgaertel, H. *J. Electrochem. Soc.* **1990**, *137*, 3626–32.

(19) For a review of these etches see Bassous, E. *Proc. Electrochem. Soc.* **1988**, *88*, 619–45.

these wafers (as described in the previous section), etching in a solution of 2-propanol and KOH produced grooves in the silicon. Figure 6b shows that there was a residual thin film on the surface. This film is probably a thin film of titanium dioxide that formed from the titanium film deposited on the silicon (to promote adhesion between gold and the substrate) before deposition of gold (See the Experimental Section). The film appears porous by SEM, and etchant seems to penetrate readily to the underlying silicon. Washing the surface with aqua regia removes the film (Figure 6c). The SEM of Figure 6c shows that the grooves are smooth on the submicrometer scale.

The process depicted in Figure 6 shows that well-defined, micrometer-scale features of silicon can be produced using a rubber stamp and simple chemical etches, without using clean-room facilities. Although the features depicted in Figure 6 are simple grooves, the production of more complex patterns is possible with more complex stamps. In addition, the features of gold produced through stamping and etching can be used as masks for dry etching process on silicon and other semiconductors.

**Electroless Deposition of Ni.** Electroless deposition is a process that deposits a metal on a surface without the requirement of an external electrical current.<sup>20</sup> The phenomenon requires a solution containing a metal ion and a reductant; the nature of the surface on which plating occurs is important. The surface is usually a metal, and often it is a catalytic surface such as palladium or a surface that has been seeded with palladium. Organic surfaces are usually resistant to electroless deposition.<sup>21</sup> We found that at high temperatures (35–60 °C), Ni would deposit on gold from an electroless plating bath (Niposit 486, Shipley Corp.). If a SAM from  $\text{HS}(\text{CH}_2)_{15}\text{CH}_3$  was present on the surface of the gold, Ni did not deposit on the derivatized regions. As with etching in cyanide, the SAM acted as a resist material for deposition of nickel.

Figure 7 shows some features produced by stamping a SAM of  $\text{HS}(\text{CH}_2)_{15}\text{CH}_3$  on gold, followed by electroless plating in the Niposit bath. Parts a–e of Figure 7 show various structures at different magnifications. Figure 7f shows a tilted micrograph; the tilt is useful for observing the morphology of the nickel film and for looking at the edge characteristics. Figure 7 indicates that the number of defects in these nickel structures appears to be greater than those found on similar surfaces of gold that had been prepared by etching a gold film, patterned with SAMs, in an  $\text{O}_2$   $\text{CN}^-$  etching solution. There are at least two factors that might contribute to the larger number of defects. First, the plating is done at temperatures between 35 and 60 °C; at these temperatures, the SAMs are probably disrupted to some degree. This disruption may allow some solution to reach the surface over regions that were derivatized. Second, during the plating process, gas bubbles formed at and attached to the surfaces. These bubbles blocked some regions from access to the plating solution, and Ni plating was not efficient over these areas.

As with the etching results, SAMs formed from  $\text{HS}(\text{CH}_2)_{15}\text{CH}_3$  or longer chain alkanethiols provided good protection. SAMs formed from shorter chain alkanethiols provided some protection, and their ability to protect the surface from deposition scaled roughly with the length of the alkanethiol chain. The terminal functionality was also important in determining the degree of protection. SAMs with hydrophobic termini such as  $-\text{CH}_3$  groups were better than SAMs with hydrophilic termini such as  $-\text{OH}$  or  $-\text{COOH}$  groups.

The patterning of SAMs using rubber stamping in combination with electroless deposition may be useful for the production of a variety of functional structures. In Figure 7, for example, gold could be selectively removed by etching to produce nickel on gold on silicon structures. The work described in this section was conducted on gold substrates with an electroless deposition bath for Ni, although comparable results were obtained with preliminary experiments using copper substrates and electroless plating baths for tin. There are also numerous other electroless plating solutions that we expect to function with these systems.<sup>22</sup> Many combinations are possible with the substrates for SAMs (gold, silver, and copper) and electroless plating baths.

**Optical Diffraction from Processes Occurring on Patterned SAMs.** *Patterned Condensation of Vapor.* When surfaces are patterned in regular arrays of hydrophobic and hydrophilic regions, condensation of water occurs preferentially on the hydrophilic regions as the temperature of the surface is decreased.<sup>23</sup> By using rubber stamps to imprint surfaces with hydrophobic and hydrophilic SAMs, we have been able to produce complex and ordered condensation figures on these surfaces.<sup>24</sup> When the size of the features are on the scale of 1–100  $\mu\text{m}$ , the corresponding ordered condensation figures can be used as optical diffraction gratings, and examination of the diffraction patterns provide a nondestructive method for characterization of such surfaces.<sup>24</sup> These condensation figures that diffract light are also potentially useful as optical, nondestructive sensors.

Figure 8 shows an optical photograph of a series of droplets condensed on a patterned surface. The surface, prepared by stamping, was hydrophobic with circular regions of diameter 2  $\mu\text{m}$  that were hydrophilic. The substrate was a thin (100 Å) layer of gold on a titanium-primed (10 Å) glass slide. This substrate was used since it was transparent to visible light, and optical microscopy required using light that was transmitted through the sample. The volume of each droplet that condensed on the hydrophilic regions was approximately  $10^{-15}$  L ( $10^{-9}$   $\mu\text{L}$ ;  $\sim 3 \times 10^{10}$  molecules). This figure also demonstrates that patterned surfaces can be characterized by examining condensation figures.

Parts a and b of Figure 9 depict a SEM of a surface patterned with SAMs and the corresponding diffraction pattern of a laser ( $\text{He:Ne}$ ,  $\lambda = 632.8$  nm) reflected from the condensation figure on the surface. This surface was prepared by using a single stamp with two lattices. The diffraction pattern, shown in Figure 9b, is that expected from a reflective surface covered with nonreflective drops whose shapes replicate those of the underlying SAMs. The diffraction pattern shows that multiple lattices and periodicities are easily distinguishable. The ability to distinguish multiple two-dimensional lattices on the surface suggests that it will be possible to place a number of independent diffracting elements on a single surface. We have shown previously that quantitative analysis of the time-dependent progression of the diffraction pattern is useful to monitor the process of condensation.<sup>24</sup> We have also demonstrated the use of this type of analysis to produce a simple humidity sensor.<sup>24</sup>

Figure 9c shows another, and convenient, method for illustrating regions differing in their wettability on pat-

(22) Ohno, Izumi *Mater. Sci. Eng., A* **1991**, *A146*, 33–49.

(20) Nakahara, S.; Okinaka, Y. *Annu. Rev. Mater. Sci.* **1991**, *21*, 93–129.

(21) Kamrava, S. J.; Soederholm, S. J. *Mater. Sci.* **1990**, *5*, 1697–702.

(23) Beysans, D.; Knobler, C. M. *Phys. Rev. Lett.* **1986**, *57*, 1433. Perrot, F.; Beysans, D. *Rev. Sci. Instrum.* **1987**, *58*, 183. Briscoe, B. J.; Galvin, K. P. *Colloids Surf.* **1991**, *56*, 263. Lopez, G. P.; Biebuyck, H. A.; Frisbie, C. D.; Whitesides, G. M. *Science (Washington, DC)* **1993**, *260*, 647.

(24) Kumar, A.; Whitesides, G. M. *Science (Washington, DC)*, in press.



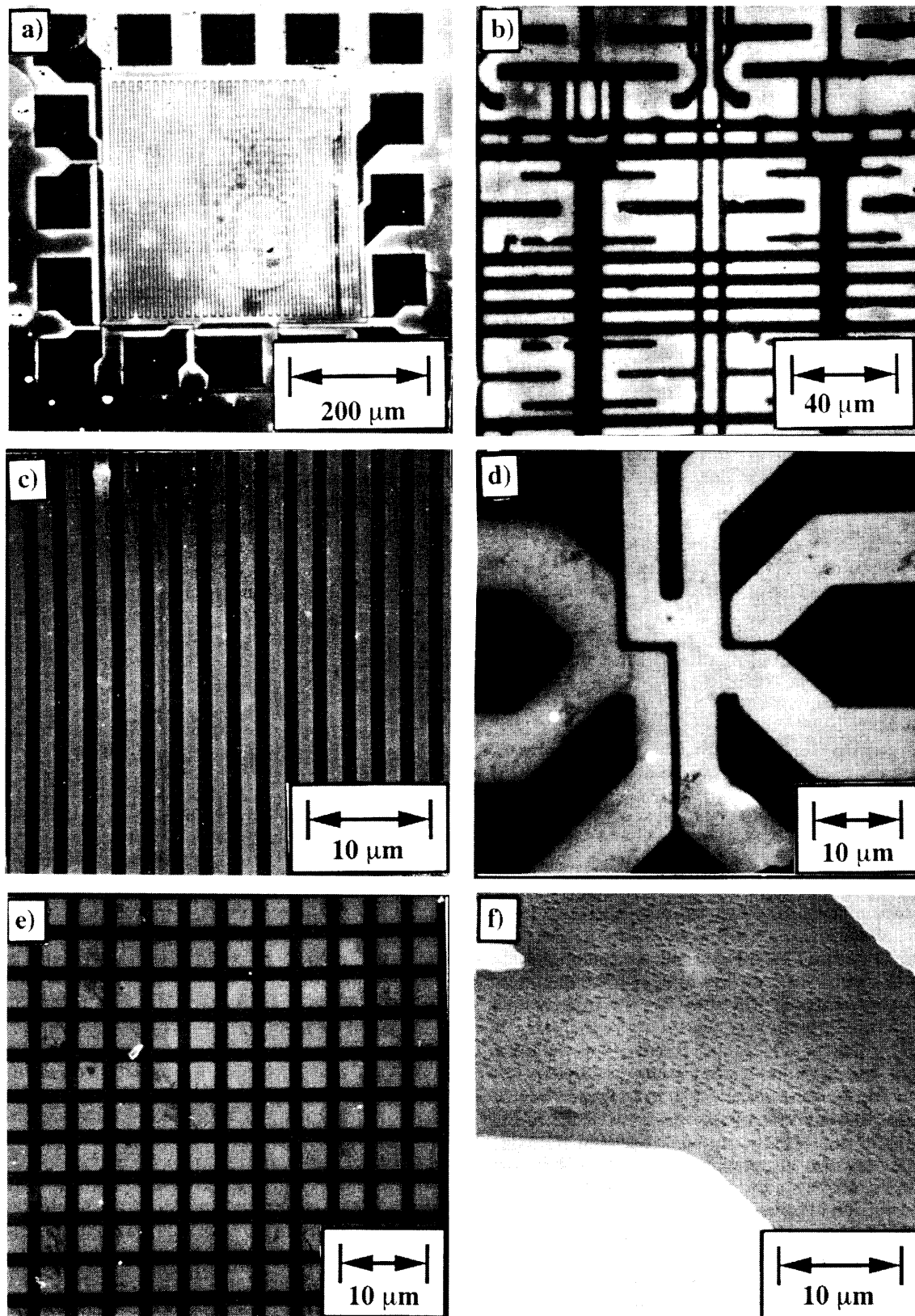


**Figure 7.** SE micrographs of patterned surfaces after nickel was deposited from an electroless plating solution. The dark regions are nickel, and the bright regions are gold. (a–e) Features of various sizes and complexities. (f) A tilted view showing the edge of a nickel layer and its morphology. See text for a discussion of the defect density.

terned surfaces: The patterned surface is placed under water. A thin layer ( $\sim 10\ \mu\text{m}$  thick) of hexadecane is placed on the water, and the sample is removed ( $\sim 1\ \text{cm/s}$ ) through the water–oil interface into air; small drops of hydrocarbon remain on the hydrophilic areas. This alternative to condensation of water on the surface (Figure 9a) is somewhat more reproducible than condensation, probably

because nonlinearities in growth of drops characteristic of condensation phenomena (due, for example, to changes in local temperature and the effective surface area of the sample) are avoided. The hydrocarbon has a low vapor pressure so that evaporation is less important; this fact extends the time of observation of the pattern and, in the limit, can be used to build structure on hydrophilic regions



**Figure 8.** Optical photograph taken of condensed drops of water that formed on a patterned surface on cooling. The surface consisted of an array of hydrophilic circles ( $2\ \mu\text{m}$  in diameter, SAM formed from  $\text{HS}(\text{CH}_2)_{15}\text{COOH}$ ) in a hydrophobic field (SAM formed by rubber stamping the adsorption of  $\text{HS}(\text{CH}_2)_{15}\text{CH}_3$ ). The substrate was a thin ( $100\ \text{\AA}$ ) layer of gold deposited on a Ti-primed ( $10\ \text{\AA}$ ) glass slide. The thin film on glass system is an optically transparent substrate that is useful for optical microscopy since light can be transmitted through the substrate.

by using appropriate prepolymers or additives to the hexadecane phase.

Figure 9d illustrates the pattern that results from simple immersion of a patterned surface in a solution of hydrocarbon in water. After gentle agitation, a stable pattern of drops of hydrocarbon cover the hydrophobic areas of the sample. This result is the consequence of the minimization of interfacial tension (the energetic cost of oil next to water is evidently lower than the cost of water next to a methyl group in hydrophobic areas of the SAM) and buoyancy of the oil in the aqueous medium. The size of the drops reflects the interplay between these two forces, the area of the hydrophobic patch, and the amount of shear experienced by the interface. Left undisturbed, the drops remain stable in this configuration for periods longer than weeks.

**Optical Diffraction as a Method of Monitoring Heterogeneous Phenomenon.** Figure 10 shows a plot of the time-dependent increase of the intensity of a first-order diffraction spot as a patterned surface corrodes in an aqueous solution of cyanide ion. A rubber stamp was used to pattern the surface with a SAM formed from  $\text{HS}(\text{CH}_2)_{15}\text{CH}_3$ . This sample was immersed in an aqueous solution containing cyanide ion. Initially, a laser beam from a He:Ne laser was reflected from the surface as a single spot. As the bare regions of gold began to dissolve, the ordered heterogeneity of the surface caused the reflected laser light to diffract. As larger areas, sampled by the laser, became heterogeneous due to the nucleation of etching, the intensity of the diffraction pattern increased. The dif-

fraction was monitored in situ without removal of the sample; the diffraction pattern was observed through the liquid. For measurement of the rate of dissolution of gold, several similar samples were placed in the solution. These samples were removed from the solution periodically, and the thickness of the remaining gold on these samples was determined using profilometry.

We emphasize that the increase of intensity of the first-order diffraction spot is due primarily to the progression of nucleation of etching and not to the dissolution of gold over areas that had commenced etching. This experiment illustrates the use of optical diffraction as a method to study the stochastic process of nucleation of corrosion. By examining higher-order diffraction spots, it may be possible to address issues relating to long range nucleation phenomenon. For example, the early appearance of higher order diffraction spots would indicate that nucleation was occurring randomly over the whole sample, rather than progressing from one single center. When done on patterned surfaces with regular periodicities, this type of analysis should be possible with other types of nucleation phenomena such as plating, polymerization, and crystallization.

These demonstrations were chosen to show the versatility of the stamping technique for patterning surfaces for the condensation of vapor, the use of condensation patterns for characterization of such surfaces, and the sensitivity of diffraction as an optical method for nondestructive characterization and process monitoring. The sensitivity of the diffraction to environmental factors such as humidity and temperature makes these systems flexible components for use in optical sensors.

**Patterned Crystallization.** Condensation on patterned surfaces can produce structures made of pure water.<sup>24</sup> These structures might also be used to carry out reactions in small volumes of water. To produce microreactors based on small drops, structures of liquids having dissolved species must be created, and condensation will not necessarily produce such systems. By slowly (less than  $5\ \text{cm/s}$ ) withdrawing a patterned substrate from a solution that wets one of the SAMs, patterns of liquid can be produced, as microdrops, microtubules, etc., without the need for condensation.

We demonstrate the microreactor principle by producing structures of solutions that contain salts and that crystallize on patterned surfaces as the liquid evaporates. Figure 11 shows examples of ionic crystals that formed when the liquid that was on the hydrophilic areas evaporated in an oven at  $65\ ^\circ\text{C}$ . Figure 11a shows the crystallization of  $\text{LiClO}_4$  on hydrophilic lines (a SAM produced from  $\text{HS}(\text{CH}_2)_{15}\text{COOH}$ ) from a methanol solution. Figure 11b,c shows the crystals that formed from aqueous solutions of  $1\ \text{M}$  cupric sulfate. In Figure 11b, the crystals form in the hydrophilic regions between hydrophobic squares (formed from a SAM produced from  $\text{HS}(\text{CH}_2)_{15}\text{CH}_3$ ). The crystals formed only on the lines oriented vertically, since the orientation with which the sample had been removed from the solution produced liquid primarily on the vertical lines. As a comparison, Figure 11c shows that the crystals formed on hydrophilic squares. Parts d and e of Figure 11 show crystallization from microtubules of water having different concentrations of potassium iodide. Solutions of  $0.1$  and  $3\ \text{M}$  KI were used in the formation of crystals shown in parts d and e of Figure 11, respectively.

Figure 12 demonstrates that the morphology of the crystals can be controlled easily by adjusting external factors. The pattern was an alternating series of hydrophilic (SAM produced from  $\text{HS}(\text{CH}_2)_{15}\text{COOH}$ ) and hy-

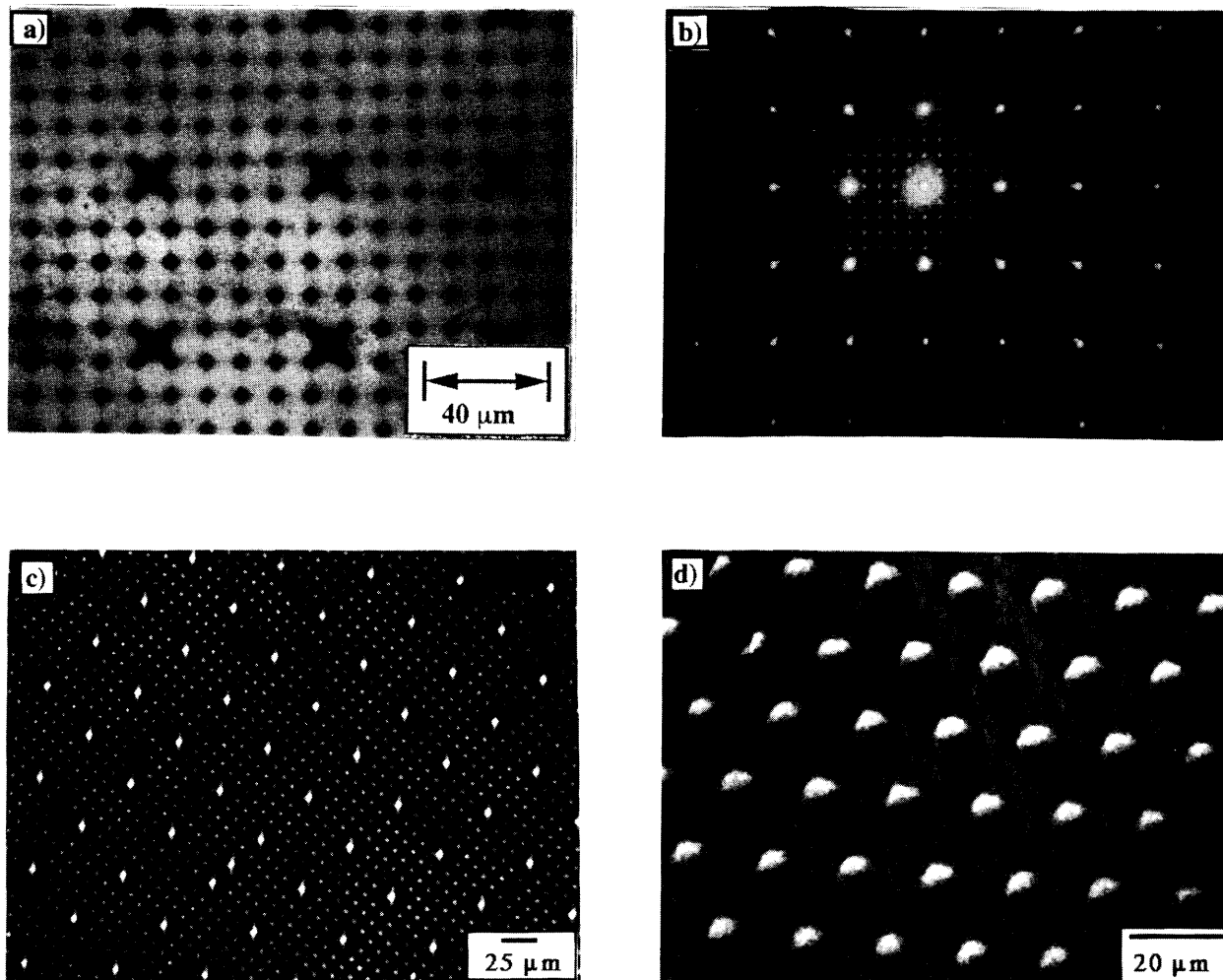


**Figure 9.** (a) SE micrograph of a surface having hydrophobic (light) and hydrophilic (dark) regions. The hydrophobic regions were formed by patterning the adsorption of  $\text{HS}(\text{CH}_2)_{15}\text{CH}_3$  using a rubber stamp. The remaining regions were rendered hydrophilic by washing with a 1 mM solution of  $\text{HS}(\text{CH}_2)_{15}\text{CO}_2\text{H}$ . The surface has two lattices with different periodicities and lateral geometries. (b) A diffraction pattern of a He:Ne laser ( $\lambda = 632.8$  nm, 1 mW) reflected off the surface after formation of a condensation figure. Note that both lattices of the surface are distinguishable in the diffraction pattern. (c) An optical photograph taken of drops of hexadecane (light areas in the figure) left behind on hydrophilic patches of a patterned surface. The surface consisted of an array of hydrophilic circles and crosses (the SAM was formed from  $\text{HS}(\text{CH}_2)_{15}\text{COOH}$ ) in a hydrophilic field (this SAM was formed first by application of a stamp of PDMS, like the one used in Figure 9a, inked with  $\text{HS}(\text{CH}_2)_{15}\text{CH}_3$  to the gold surface). The SAM was formed on a gold substrate similar to Figure 8. The photograph was taken with light in transmission through this film within 30 s of emergence of the substrate from a phase separated solution of 100  $\mu\text{L}$  of hexadecane in 10 mL of water. (d) An optical photograph of drops of hexadecane wetting hydrophobic areas of a patterned surface under water. The surface consisted of an array of hydrophobic circles (this SAM was formed first by application of a PDMS stamp inked with  $\text{HS}(\text{CH}_2)_{15}\text{CH}_3$  to the gold surface) in a hydrophilic field (the SAM was formed from  $\text{HS}(\text{CH}_2)_{15}\text{COOH}$ ). The SAM was formed on a gold substrate similar to Figure 8. The photograph was taken with light in transmission through this film while the patterned gold film remained in the aqueous portion of solution of 100  $\mu\text{L}$  of hexadecane in 10 mL of water. The microscope objective lens was also immersed in this phase during capture of the image.

drophobic (SAM produced from  $\text{HS}(\text{CH}_2)_{15}\text{CH}_3$ ) lines. The liquid was an aqueous solution of 1 M  $\text{K}_3\text{Fe}(\text{CN})_6$ . Figure 12a shows the morphology of the crystals that formed when the solution evaporated in an oven at 95 °C. The morphologies and shapes of the crystals were different when the liquid was allowed to evaporate in air (relative humidity of 60%) at 22 °C. The rates of evaporation, controlled by the temperature and relative humidity of the environment, and the concentration of salt in the liquid should allow for the formation of crystals of different sizes and morphologies. Figure 12c demonstrates that in some cases crystals of very high aspect ratio (1.2 mm length, 10  $\mu\text{m}$  width) could be produced. It may be possible to form single crystals of complex shapes and patterns through this technique.

This technique of localizing small volumes of liquid also opens up the possibility of conducting chemical and biochemical reactions in extensive arrays of microreactors. With such small volumes, small numbers of reactant

species such as enzymes, cells, or even microorganisms could be isolated reproducibly. More complex systems, where aqueous structures are generated on immersion of patterned samples in nonaqueous environments (or *vice versa*), can also be formed.

**Substrates for Scanning Probe Microscopies.** It would be useful to produce well-defined surfaces that could be used in conjunction with scanning probe microscopies to study tribological interactions. In addition, interpretation, of AFM and scanning tunneling microscopic (STM) images of heterogeneous surfaces comprising SAMs has often been ambiguous, since well-defined regions could not be prepared easily.<sup>25</sup> By use of the printing techniques described here, patterned surfaces can now be produced

(25) Overney, R. M.; Meyer, E.; Frommer, J.; Brodbeck, D.; Luethi, R.; Howald, L.; Guentherodt, H. J.; Fujihira, M.; Takano, H.; Gotoh, Y. *Nature (London)* **1993**, 359, 133–5. Overney, R. M.; Meyer, E.; Frommer, J.; Guentherodt, H. J.; Decher, G.; Reibel, J.; Sohling, U. *Langmuir* **1993**, 9, 341–6.

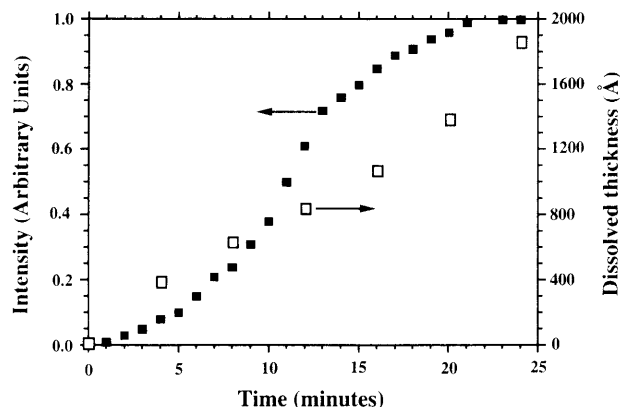


**Figure 10.** Increase of intensity (black boxes) of a first-order diffraction spot as a patterned surface of gold corroded in an aqueous solution containing 1 M KOH and 1 mM KCN. The solution was left open to the atmosphere. The increase in intensity is a measure of the rate of nucleation of the etch, not the dissolution of gold. The open boxes show the rate of dissolution of gold as measured by profilometry.

quickly and reproducibly. As an example of the use of these patterned surfaces, Figure 13 shows an atomic force microscope (AFM, the image was obtained in the lateral force mode) image and a corresponding scanning electron micrograph of a patterned surface. A SAM from HS-(CH<sub>2</sub>)<sub>15</sub>CH<sub>3</sub> was formed by stamping, followed by derivatization of the bare gold with HS(CH<sub>2</sub>)<sub>15</sub>COOH. This figure illustrates the ability of the lateral force mode of imaging to distinguish between two SAMs differing only in terminal functionality. The contrast in the AFM image is probably due to the forces felt by the probe tip from interaction with surface functionalities, adsorbed adventitious contaminants, and water.

One surface with several microscopic areas (micrometer scale) was produced, although the image was not obtained with atomic resolution. Interpretation of higher-resolution images may therefore be simpler than those that require several exchanges of samples and several approaches to the surfaces.

### Conclusions

We have described a method for patterning the adsorption of alkanethiolates on surfaces of gold using an elastomeric stamp. Key advantages of this method—simplicity and ruggedness—are underscored by the experiments described in this paper: With the exception of fabricating the masters, all experiments were conducted in a conventional chemical laboratory. No routine access to photolithography equipment or clean rooms was necessary. This technique has been used to produce substrates for several different applications.

The simplicity of this technique provides great flexibility and potential for many other applications. In addition to the applications discussed in this paper, stamping has found some use in biological areas.<sup>26</sup> By use of a stamp, surfaces with islands that are adhesive toward proteins surrounded by nonadhesive areas have been prepared. These surfaces are useful for the nonspecific adsorption of several proteins in patterns. Such surfaces have also been useful for the attachment, control of shape and morphology, and control of function of mammalian cells. These procedures provide an alternative to photolithographic techniques to produce patterned substrates for

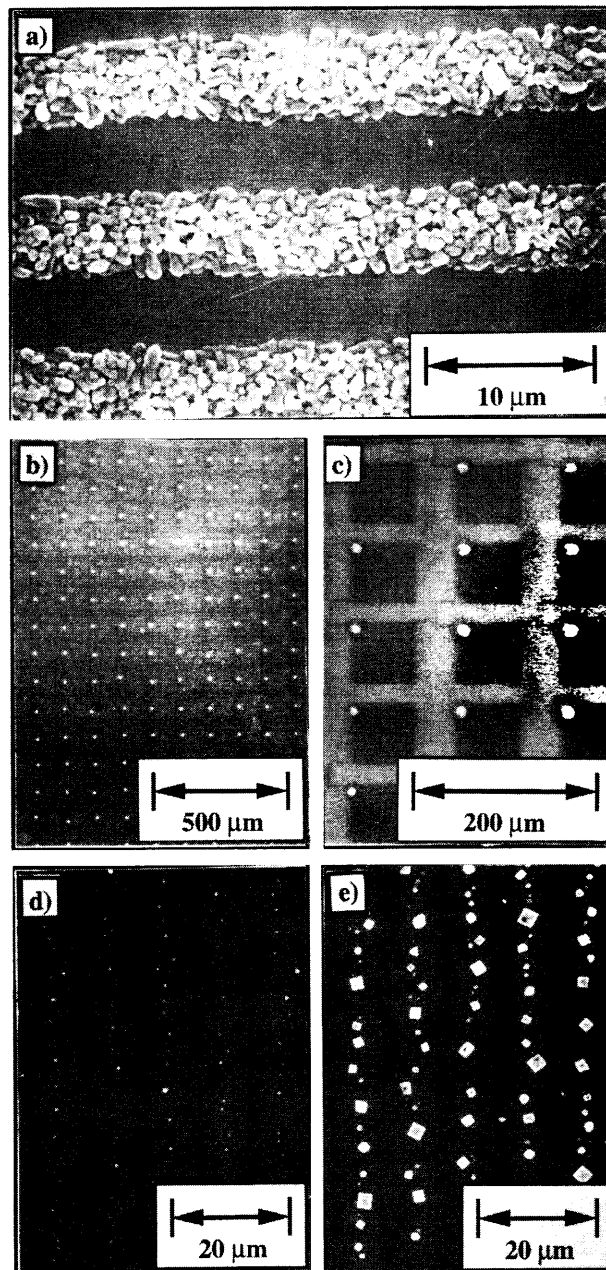


**Figure 11.** Patterned crystallization. (a) LiClO<sub>4</sub> crystallized from a saturated solution of methanol that formed on the hydrophilic (SAM formed from HS(CH<sub>2</sub>)<sub>15</sub>COOH) regions of a patterned substrate. The hydrophobic regions were formed by rubber stamping the adsorption of HS(CH<sub>2</sub>)<sub>15</sub>CH<sub>3</sub>. (b, c) Arrays of crystals of CuSO<sub>4</sub> that formed on hydrophilic regions from 1 M, aqueous solutions. Crystals that formed from patterned solutions of KI are shown in parts d and e. The concentration of KI was 0.1 and 3 M for the solutions used to prepare parts d and e, respectively. The liquid in each case was evaporated in an oven at 65 °C.

biological systems. Other applications include patterned electrochemical deposition of metals, semiconductors, and conducting polymers, patterned localization of polymers, and others.

### Experimental Section

**Materials.** Gold (99.999%), copper (99.999%), silver (99.999%) and titanium (99.99%) were obtained from Materials Research Corp. (Orangeburg, NY). Stamps were made of poly-(dimethylsiloxane) sold by Dow-Corning (Midland, MI) as SYLGARD Silicone Elastomer-184. Silicon wafers of (100) orientation were obtained from Silicon Sense (Nashua, NH). The electroless plating bath for nickel, Niposit 486, was obtained

(26) Singvi, R.; Kumar, A.; Lopez, G. P.; Stephanopoulos, G. N.; Wang, D.; Whitesides, G. M.; Ingber, D. E. Submitted for publication in *Science*.

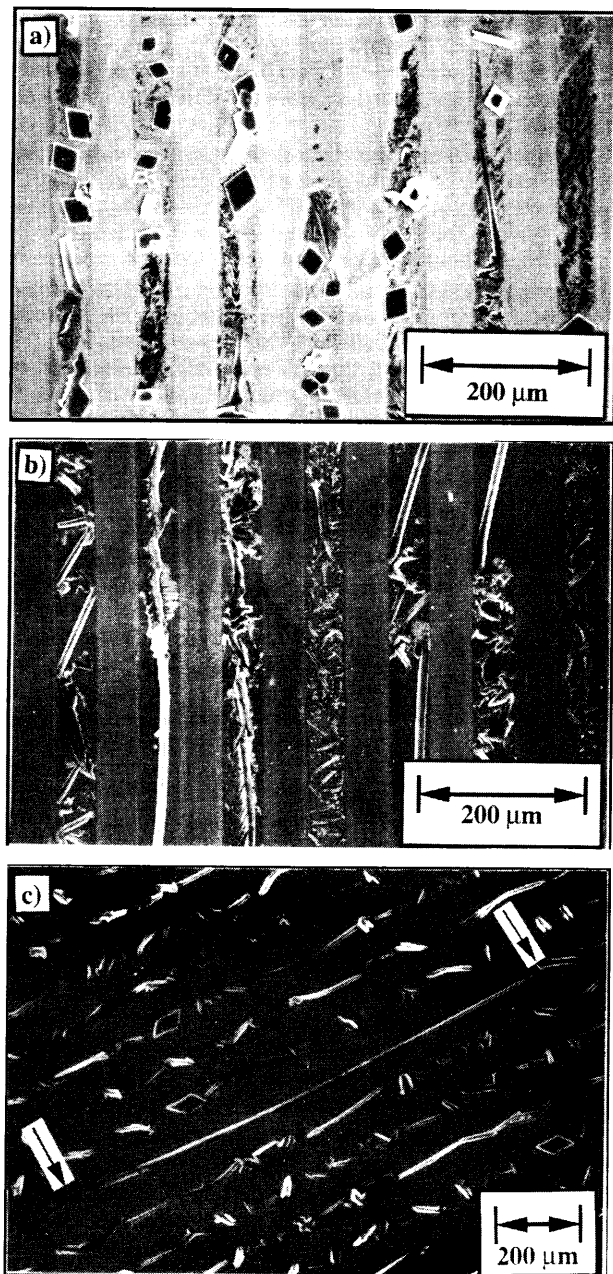


**Figure 12.** Demonstration of the control of morphology and shape of formation of crystals. A surface with alternating hydrophobic (SAM formed by rubber stamping the adsorption of  $\text{HS}(\text{CH}_2)_{15}\text{CH}_3$ ) and hydrophilic (SAM formed from  $\text{HS}(\text{CH}_2)_{15}\text{COOH}$ ) lines was formed. Microtubules of water containing 1 M  $\text{K}_3\text{Fe}(\text{CN})_6$  were formed on the hydrophilic regions. (a) The liquid was allowed to evaporate in an oven at  $65^\circ\text{C}$ . (b) The liquid was allowed to evaporate in air at  $22^\circ\text{C}$  (relative humidity of  $60\%$ ). In some cases, crystals of high aspect ratio (denoted by arrows) are observed.

from Shipley Co. (Marlborough, MA), and the electroless plating bath for tin was obtained from Kepro Circuit Systems (Fenton, MO). Absolute ethanol ( $\text{CH}_3\text{CH}_2\text{OH}$ ) was obtained from Pharmco (Weston, MO). Hexadecanethiol ( $\text{HS}(\text{CH}_2)_{15}\text{CH}_3$ ), lithium perchlorate ( $\text{LiClO}_4$ ), squaric acid (3,4-dihydroxy-3-cyclobutene,  $\text{C}_4\text{H}_2\text{O}_4$ ), ferric chloride ( $\text{FeCl}_3$ ) and potassium thiocyanate ( $\text{KSCN}$ ) were obtained from Aldrich Chemical Co. (Milwaukee, WI). Concentrated hydrochloric acid ( $\text{HCl}$ ), concentrated nitric acid ( $\text{HNO}_3$ ), potassium chloride ( $\text{KCl}$ ), iodine ( $\text{I}_2$ ), cupric sulfate ( $\text{CuSO}_4$ ), and potassium ferricyanide ( $\text{K}_3\text{Fe}(\text{CN})_6$ ) were obtained from Mallinkrodt (Paris, KY). Hexane ( $\text{C}_6\text{H}_{12}$ ), isooctane ( $(\text{CH}_3)_3\text{CCH}_2\text{CH}(\text{CH}_3)_2$ ), toluene ( $\text{C}_7\text{H}_8$ ), isopropyl alcohol ( $(\text{CH}_3)_2\text{CHOH}$ ), methanol ( $\text{CH}_3\text{OH}$ ), hydrogen peroxide ( $\text{H}_2\text{O}_2$ ,  $30\%$ ), sodium thiosulfate ( $\text{Na}_2\text{S}_2\text{O}_3$ ), potassium hydroxide ( $\text{KOH}$ ), and potassium cyanide ( $\text{KCN}$ ) were obtained from Fisher Scientific (Fair Lawn, NJ). Potassium iodide ( $\text{KI}$ ) was obtained from Merck

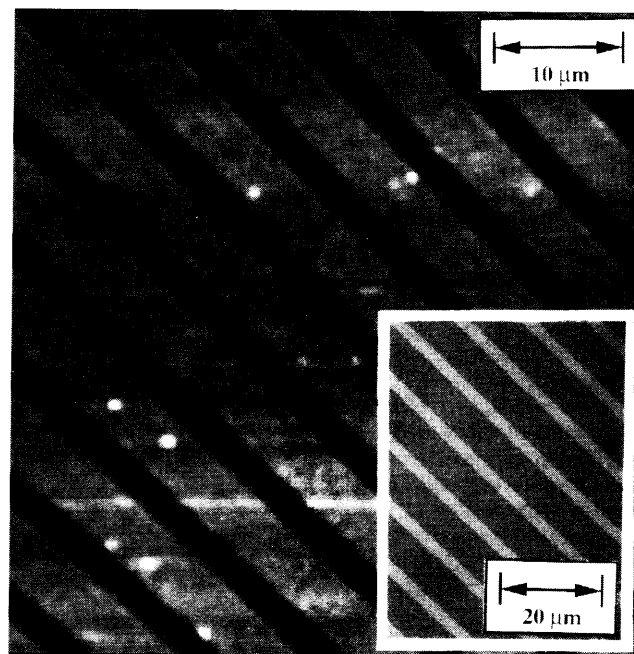


**Figure 13.** Microscopic images of a pattern of alternating lines formed from SAMs of  $\text{HS}(\text{CH}_2)_{15}\text{CH}_3$  and  $\text{HS}(\text{CH}_2)_{15}\text{COOH}$ . The main figure shows an AFM image taken in the lateral force mode of the series of lines. A silicon nitride cantilever was scanned across the surface at a rate of  $100\ \mu\text{m/s}$  and with a constant force of  $0.1\ \text{nN}$ . Changes in the lateral force on the substrate were detected as differences between the photocurrent from the left and right halves of the photodetector. The  $-\text{CH}_3$  terminated regions appear dark in the AFM image since the force felt by the tip as it rasters across these regions is lower than that felt over the  $-\text{COOH}$  terminated regions. The inset is a SEM of low free energy lines of a  $-\text{CH}_3$  terminated SAM (light) spaced by lines of a  $-\text{COOH}$  terminated SAM (dark). The demonstration shows that these surfaces can be used for microtribological studies. The bright spots are dust particles on the surface.

(Rahway, NJ), and sodium chloride was obtained from EM Science (Gibbstown, NJ). All of these materials were used as obtained from the manufacturers. The preparations for other alkanethiols ( $\text{HS}(\text{CH}_2)_{10}\text{CH}_2\text{OH}$  and  $\text{HS}(\text{CH}_2)_{15}\text{COOH}$ ) are reported elsewhere.<sup>5</sup>

**Preparation of Substrates.** Gold films ( $100\ \text{\AA}$  to  $1\ \mu\text{m}$ ) were deposited by electron beam evaporation on glass slides or silicon wafers that had been primed with titanium ( $5\text{--}50\ \text{\AA}$ ) to promote adhesion between silicon oxide and gold.

**Preparation of Stamps and Formation of Monolayers.** Most of the masters for fabrication of stamps were prepared by using conventional photolithography as described elsewhere. Good stamps were fabricated from corrugations made in a variety of photoresists, metals, or polymers. Alternatively, transmission electron microscopy grids provided useful masters. Stamps with large features ( $0.5\ \text{mm}$ ) were also fabricated from masters that were prepared by cutting grooves in aluminum blocks with a silicon carbide disk saw. In principle, any surface with corrugations of appropriate size could be used as masters. An important consideration was that the aspect ratio (the ratio of the width to the height) of the corrugations needed to be close to unity, preferably in the range between  $0.5$  and  $2$ . This was important so that there would not be significant distortion of the features during stamping.

The master was placed in a plastic or glass petri dish, and a  $10:1$  ratio (w:w or v:v) mixture of SYLGARD silicone elastomer 184 and SYLGARD silicone elastomer 184 curing agent was poured over it. The polymer was allowed to cure overnight at room temperature or it was placed in an oven ( $65^\circ\text{C}$ ,  $1$  to  $2\ \text{h}$ ) after setting at room temperature for approximately  $1\ \text{h}$ . After removal from the oven the polymer was allowed to cool to room temperature. A razor blade was used to cut sections of the polymer. The thickness of the stamp ( $1\text{--}3\ \text{mm}$ ) was not critical. These sections were peeled from the master. The peeled sections were washed several times with ethanol and heptane (the last



washing was with ethanol) and dried with a flowing stream of nitrogen before being used as a stamp.

The ink formulation was a 0.1–10 mM solution of the desired alkanethiol in either ethanol or diethyl ether. Other ink formulations based on solvents such as hexane, isooctane, or toluene did not produce good results (perhaps because the PDMS did not swell with these inks).

Inking of the stamp was done in one of several ways. First, the ink was poured onto a piece of absorbent paper, and the stamp was touched to the paper. Second, a Q-tip was soaked with the ink and was rubbed across the face of the stamp. Third, the ink was directly poured onto the stamp. In all cases, the stamp swelled with the ink. The gross liquid was dried in a stream of flowing nitrogen. The stamp could be used several times before requiring more ink.

After inking, the stamp was placed gently on the substrate. Very light pressure was applied by hand to ensure contact between the stamp and substrate. The stamp could be removed immediately or removed after several hours without any noticeable change in resolution of features. After removal of the stamp, another stamp with the same or other alkanethiol could be used to stamp another pattern. In this way the surface could be imprinted with multiple SAMs. The surface could also be washed with a solution containing another alkanethiol to derivatize regions not imprinted by stamping.

**Procedures.** Etching of gold was done at room temperature, in a Pyrex beaker that was open to the laboratory ambient. The solution used for etching contained KOH (1 M) and KCN (0.1 mM to 0.1 M). The solution was stirred during etching. Oxygen was continuously bubbled through the solution during etching. Alternatively, the solution was saturated by bubbling oxygen previous to etching. Fresh solutions were made for some of the experiments, although the solutions lasted for weeks without noticeable degradation in etching behavior. The best results were obtained for substrates that had been freshly (less than 1 day old) prepared.

For etching with ferricyanide, no bubbling oxygen was necessary, but the solution was cooled to 2–5 °C by immersing the beaker in a dry ice bath. The concentration of ferricyanide was 0.1 mM. All other etch experiments described in Table 1 were conducted in Pyrex beakers at room temperature. The solutions were stirred, and they were left exposed to the laboratory ambient. When oxygen was used as the oxidant, it was bubbled through the solution throughout the etching procedure. When other oxidants were used, appropriate amounts were added to the solution.

Etching of silicon was done at room temperature in a Pyrex or polyethylene container that was open to the laboratory

ambient, in an aqueous solution of KOH (2–6 M) with 2-propanol (15% by volume). The solution was stirred vigorously to keep the aqueous and nonaqueous layers from separating. Occasionally, 2-propanol was added to replenish the amount that had evaporated.

The Niposit 486 bath, for electroless deposition of nickel, was prepared as described in the product literature from Shipley Co. The patterned substrate was placed in the plating bath that was stirred, open to the laboratory ambient, and heated on a hot plate. The solutions were prepared fresh for each experiment.

For measurements of the intensity of spots diffracted from condensation figures or corroding surfaces, a United Detector Technologies UDT-UV50 silicon PIN photodiode was used. The diode was short-circuited through a 100-k $\Omega$  resistor, and the voltage drop across the resistor was monitored with a digital multimeter. The light source was a 5 mW He:Ne laser ( $\lambda = 632.8$  nm) obtained from Edmund Scientific (Barrington, NJ).

**Instrumentation.** Scanning electron microscopy and energy dispersive X-ray spectroscopy were done on a JEOL JSM-6400 scanning microscope (Tokyo, Japan). Images were acquired in the secondary electron imaging mode.

Atomic force microscopy was done on a Topometric TMX 2010 scanning probe microscope (Mountain View, CA). The images were obtained by using a cantilever made from silicon nitride in constant contact with the surface. The cantilever was scanned across the substrate at a rate of 100  $\mu\text{m/s}$  and with a constant force of 0.1 nN; data were collected in the forward part of the scan. Changes in the lateral force on the substrate were detected as differences between the photocurrent from the left and right halves of the photodetector. We found no change in these images even after repeated scanning in one area.

Profilometry measurements were made using a Tencor Instruments Alpha-step 2000 (Mountain View, CA) scanning profilometer. A silicon carbide tip with a radius of curvature of 12.5  $\mu\text{m}$  was the probe.

**Acknowledgment.** This work was supported in part by the Office of Naval Research and ARPA. Electron microscopy and photolithography were performed using instrumentation in the Materials Research Laboratory at Harvard University. We thank Henry Smith of the Massachusetts Institute of Technology for supplying some substrates that were used as masters for the fabrication of stamps; Dr. Jane Alexander arranged that others be made available.